NASA TECHNICAL MEMORANDUM

NASA TM X-885

NASA TM X-885

EFFECTS OF BOOSTER FINS ON STATIC STABILITY CHARACTERISTICS OF A 0.02-SCALE MODEL OF THE TITAN III LAUNCH VEHICLE WITH THE DYNA-SOAR GLIDER AND A BULBOUS NOSE AT MACH NUMBERS FROM 1.60 TO 3.50

By Lloyd S. Jernell and C. Donald Babb
Langley Research Center
Langley Station, Hampton, Va.

NATIONAL AERONAUTICS AND SPACE ADMINISTRATION • WASHINGTON, D. C. • OCTOBER 1963

TECHNICAL MEMORANDUM X-885

EFFECTS OF BOOSTER FINS ON STATIC STABILITY CHARACTERISTICS OF A 0.02-SCALE MODEL OF THE TITAN III LAUNCH VEHICLE WITH THE DYNA-SOAR GLIDER AND A BULBOUS NOSE AT MACH NUMBERS FROM 1.60 TO 3.50

By Lloyd S. Jernell and C. Donald Babb

Langley Research Center
Langley Station, Hampton, Va.

NATIONAL AERONAUTICS AND SPACE ADMINISTRATION

NATIONAL AERONAUTICS AND SPACE ADMINISTRATION

TECHNICAL MEMORANDUM X-885

EFFECTS OF BOOSTER FINS ON STATIC STABILITY CHARACTERISTICS OF A 0.02-SCALE MODEL OF THE TITAN III LAUNCH VEHICLE WITH THE DYNA-SOAR GLIDER AND A BULBOUS NOSE AT MACH NUMBERS FROM 1.60 TO 3.50*

By Lloyd S. Jernell and C. Donald Babb

SUMMARY

15951

A wind-tunnel investigation has been conducted at Mach numbers from 1.60 to 3.50 to determine the effects of several booster-fin configurations on the static longitudinal and lateral stability characteristics of an 0.02-scale model of the Titan III launch vehicle with the Dyna-Soar glider. Tests were also performed with a fin configuration in conjunction with a bulbous nose at Mach numbers of 1.60 and 2.00.

The effectiveness of the pitch fins in producing normal force and pitching moment appears to vary linearly with fin area, indicating no significant interference effects due to launch vehicle, glider, or bulbous nose. The configurations with the Dyna-Soar glider and the small and large pitch fins each exhibit a decrease in longitudinal stability with increasing Mach number, the rate of change being about the same for both configurations. The addition of the medium yaw fins (four panels, two upper and two lower) has little effect on the rolling moment due to sideslip in comparison with the finless configuration. However, the large yaw fins (two panels, lower only) provide more positive values of rolling moment due to sideslip.

AUTHOR

INTRODUCTION

Launch vehicles designed to provide the required performance for any space mission in the foreseeable future are presently being developed by the National Aeronautics and Space Administration. One method of meeting the demand for relatively high launch-vehicle performance during the interim time period before these larger vehicles are operational is by additional staging of present hardware. In order to fulfill the current need for a launch vehicle capable of orbiting a spacecraft, such as the Dyna-Soar glider, a liquid-propellant Titan II vehicle has been modified (Titan III core) and staged with two coplanar solid-propellant

*Title, Unclassified.

strap-on auxiliary boosters. The solid-propellant boosters comprise the first stage of the modified vehicle designated Titan III.

The amount of thrust vector control available from the first-stage boosters of the Titan III is presently uncertain. However, it is believed that fins will be required to obtain satisfactory stability characteristics, especially for the Dyna-Soar glider type of spacecraft. Accordingly, an investigation has been performed to determine the effect of several booster-fin arrangements on the static stability characteristics of a 0.02-scale model of a configuration of the Titan III launch vehicle and Dyna-Soar glider. Additional tests were performed on the Titan III model with a bulbous nose.

The investigation was performed in the Langley Unitary Plan wind tunnel at Mach numbers from 1.60 to 3.50, angles of attack from about -9° to 9°, and angles of sideslip from about -8° to 8°. The Reynolds number was 2.7×10^6 per foot.

COEFFICIENTS AND SYMBOLS

The data are presented about the body-axis system (fig. 1). The moment coefficients are referenced to a point on the core center line 4.28 inches forward of the core base. The symbols used in this report are as follows:

A core cross-sectional area, 0.0315 sq ft

C_A axial-force coefficient, $\frac{\text{Axial force}}{qA}$

$C_{A,b}$ base axial-force coefficient, $\frac{\text{Base axial force}}{qA}$

$C_{A,o}$ axial-force coefficient at zero normal force

C_l rolling-moment coefficient, $\frac{\text{Rolling moment}}{qAd}$

C_{l_β} rolling-moment derivative ($\beta \approx 0^\circ$), $\frac{\partial C_l}{\partial \beta}$, per deg

C_m pitching-moment coefficient, $\frac{\text{Pitching moment}}{qAd}$

$C_{m_{C_N}}$ longitudinal stability parameter, $\frac{\partial C_m}{\partial C_N}$

C_N normal-force coefficient, $\frac{\text{Normal force}}{qA}$

C_{N_α} slope of normal-force curve through $\alpha \approx 0^\circ$, $\frac{\partial C_N}{\partial \alpha}$, per deg

C_n yawing-moment coefficient, $\frac{\text{Yawing moment}}{qAd}$

C_{n_β} directional-stability parameter ($\beta \approx 0^\circ$), $\frac{\partial C_n}{\partial \beta}$, per deg

C_Y side-force coefficient, $\frac{\text{Side force}}{qA}$

C_{Y_β} side-force derivative ($\beta \approx 0^\circ$), $\frac{\partial C_Y}{\partial \beta}$, per deg

d core diameter, 2.403 in.

M free-stream Mach number

q free-stream dynamic pressure

X,Y,Z body axes

α angle of attack, referred to core center line, deg

β angle of sideslip, referred to core center line, deg

Model component designation:

B Titan III core plus solid-propellant boosters

F_{P1} small pitch fins (two panels), Area per panel = 11.52 sq in.

F_{P2} large pitch fins (two panels), Area per panel = 20.16 sq in.

F_{Y1} small yaw fins (four panels), Area per panel = 1.85 sq in.

F_{Y2} medium yaw fins (four panels), Area per panel = 3.24 sq in.

F_{Y3} large yaw fins (two panels, bottom only), Area per panel = 3.93 sq in.

P_D Dyna-Soar glider including orbital transition section

P_N bulbous nose (replaces glider and orbital transition section)

APPARATUS AND METHODS

Model

The Titan III model was tested in combination with the Dyna-Soar glider (fig. 2(a)) and a bulbous nose (fig. 2(b)). The drawings and dimensions of the two sets of booster pitch fins and the three sets of booster yaw fins are presented in figures 2(c) and 2(d), respectively. It should be emphasized that each set of small and medium yaw fins consisted of four panels, an upper and a lower panel for each solid-propellant booster, whereas the set of large yaw fins consisted of the two lower panels only.

A photograph of the test-section installation of the model of the Titan III launch vehicle with the Dyna-Soar glider and the small pitch and yaw fins is presented as figure 3.

Tunnel

The investigation was conducted in both the low and the high Mach number test sections of the Langley Unitary Plan wind tunnel, which is of the variable-pressure, return-flow type of wind tunnel. The test sections are 4 feet square by approximately 7 feet in length. Asymmetric sliding-block-type nozzles lead to the test sections and permit a continuous variation of Mach number from about 1.5 to 2.9 and 2.3 to 4.7 in the low and high Mach number test sections, respectively.

Measurements

Forces and moments acting on the model were measured by means of a sting-supported, six-component, strain-gage balance mounted within the model center body or core.

Base pressures were measured by means of static-pressure orifices located at the bases of the core and the boosters.

Tests

Aerodynamic characteristics in pitch were obtained through an angle-of-attack range from approximately -9° to 9° at $\beta = 0^\circ$. Aerodynamic characteristics in sideslip were obtained through an angle-of-sideslip range from approximately -8° to 8°. The dewpoint, measured at stagnation pressure, was maintained low enough to insure negligible condensation effects. Other test conditions were as follows:

M	Stagnation pressure, lb/sq ft abs	Dynamic pressure, lb/sq ft	Reynolds number per foot	Stagnation temperature, ^{o}F
1.60	1,457	614	2.7×10^{6}	125
2.00	1,688	604	2.7	125
2.50	2,282	585	2.7	150
3.00	2,982	512	2.7	150
3.50	3,895	438	2.7	150

Boundary-layer transition strips were placed on the glider and booster fins at approximately the 5-percent local chord and on the glider wings at about the 10-percent local chord. Transition strips were also used on the noses of the glider and the solid-propellant boosters and on the bulbous nose. All transition strips were approximately 1/16 inch in width and were composed of No. 60 carborundum grains embedded in plastic adhesive.

CORRECTIONS AND ACCURACIES

The axial-force coefficients have been adjusted to a condition of free-stream static pressure at the bases of the model. The base axial-force coefficients used in this adjustment are presented in figure 4.

The angles of attack and sideslip have been corrected for wind-tunnel flow misalinement and model support-system deflection under aerodynamic load.

The estimated accuracies of the measured data, based on instrument calibration and data repeatability, are as follows:

C_N . . . . . ±0.20
C_A . . . . . ±0.10
C_m . . . . . ±0.50
C_l . . . . . ±0.05
C_n . . . . . ±0.50
C_Y . . . . . ±0.20

The Mach number accuracy was estimated to be within ±0.015. The estimated accuracy of angles of attack and sideslip was within ±0.1.

PRESENTATION OF RESULTS

The results of the investigation are presented in the following figures:

DISCUSSION OF RESULTS

The effects of fins, glider, and bulbous nose on the aerodynamic characteristics in pitch of the Titan III model are shown in figure 5. All test configurations exhibit a relatively linear variation of normal-force and pitching-moment coefficients with angle of attack throughout the test Mach number range. The effectiveness of the pitch fins in producing normal force and pitching moment appears to vary linearly with fin area, indicating no significant interference effects due to launch vehicle, glider, or bulbous nose.

A summary of the aerodynamic characteristics in pitch is presented in figure 6. The normal-force-curve slope C_{N_α} is seen to decrease with increasing Mach number and with decreasing fin size, as would be expected.

The level of stability presented herein does not correspond to that expected in flight since the expected flight center of gravity is somewhat forward of the model moment center. However, the variations of $C_{m_{C_N}}$ presented in figure 6 are indicative of the relative effects of fins, glider, and bulbous nose. For the configuration with the Dyna-Soar glider and no fins, the aerodynamic center moves rearward approximately 1/2 diameter as Mach number is increased from 1.6 to 3.5. This increase in stability with Mach number is due, of course, to the concurrent decrease in the glider C_{N_α}. The addition of the small pitch fins F_{P1} results in a rearward movement of the aerodynamic center of about 3 diameters at $M = 1.6$. However, as Mach number is increased, the loss in stability due to decreasing fin effectiveness overshadows the stability gain due to the glider and the result is an overall loss in stability such that at $M = 3.5$ the addition of the small fins causes a rearward aerodynamic-center movement of only about $1\frac{1}{2}$ diameters. The large pitch fins F_{P2} provide an increase in static margin of approximately 3/4 diameter over that of the small fins throughout the test Mach number range.

For the range $1.6 \leqq M \leqq 2.0$ the configuration with the bulbous nose and small pitch fins exhibits about the same magnitude of stability as does the configuration with the glider and large fins.

The aerodynamic characteristics in sideslip are presented in figures 7 to 11. The data, in general, exhibit a relatively linear variation with angle of sideslip. The sideslip characteristics for only those configurations which were investigated at several angles of attack are summarized in figure 12. For each configuration the rolling-moment derivative C_{l_β} decreases linearly as angle of attack is increased from about -6° to 6°. A comparison of the data for configurations $P_D B$ and $P_D B F_{P2} F_{Y2}$ (figs. 12(a) and 12(b)) indicates that the addition of the fins has little effect on C_{l_β} and, as expected, increases the level of directional stability. With the large yaw fins (lower panels only) there is an increase in C_{l_β} throughout the angle-of-attack range (compare figs. 12(a) and (c)) and C_{n_β} is slightly less than that for the configuration with medium yaw fins (figs. 12(b) and (c)).

CONCLUSIONS

An investigation has been conducted to determine the static longitudinal and lateral stability characteristics of the Titan III launch vehicle with several booster-fin configurations in combination with the Dyna-Soar glider and a bulbous nose. From the results the following conclusions are indicated:

1. The effectiveness of the pitch fins in producing normal force and pitching moment appears to vary linearly with fin area, indicating no significant interference effects due to launch vehicle, glider, or bulbous nose.

2. The configurations with the Dyna-Soar glider and the small and large pitch fins each exhibit a decrease in longitudinal stability with increasing Mach number, the rate of change being about the same for both configurations.

3. The addition of the medium yaw fins (four panels, two upper and two lower) has little effect on the rolling moment due to sideslip in comparison with the finless configuration. However, the large yaw fins (two panels, lower only) provide more positive values of rolling moment due to sideslip.

Langley Research Center,
National Aeronautics and Space Administration,
Langley Station, Hampton, Va., June 6, 1963.

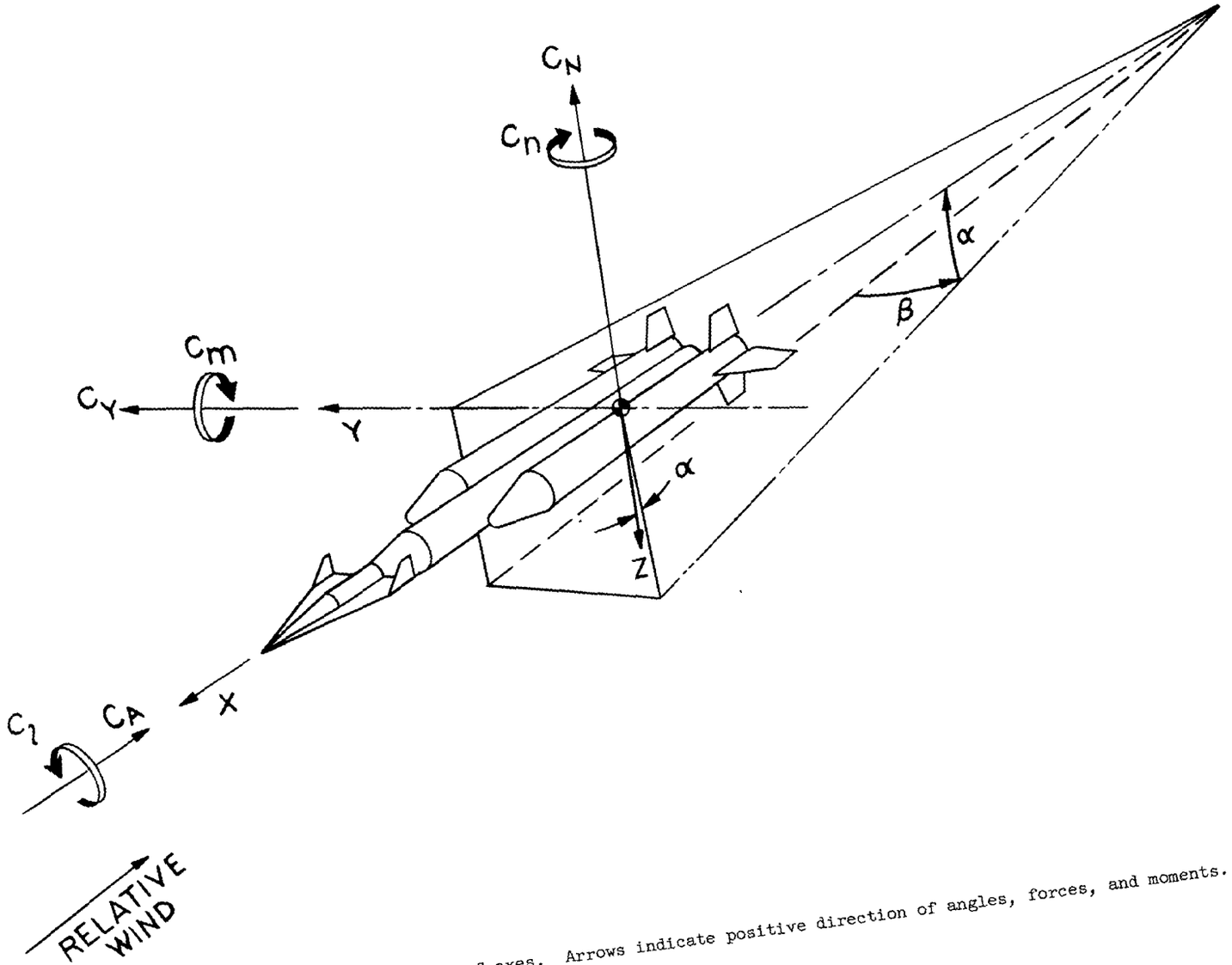

Figure 1.- System of axes. Arrows indicate positive direction of angles, forces, and moments.

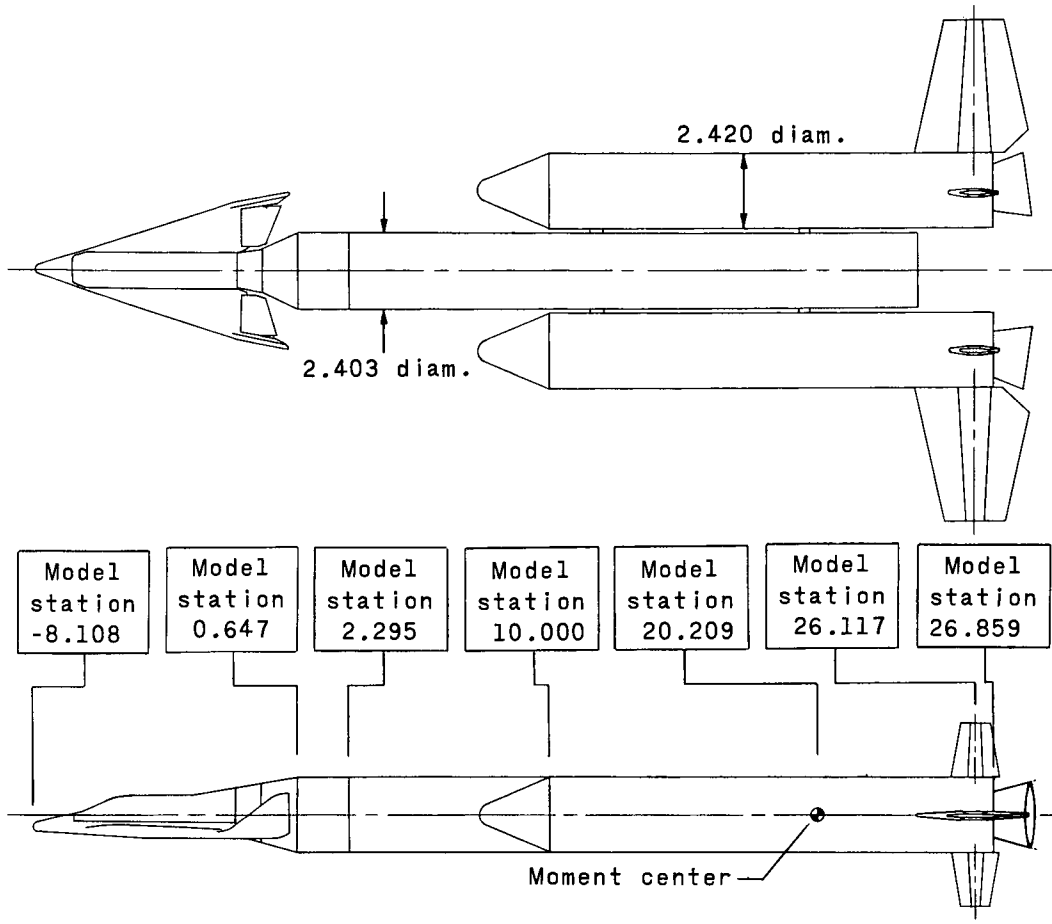

(a) Launch vehicle with Dyna-Soar glider and small pitch and yaw fins.

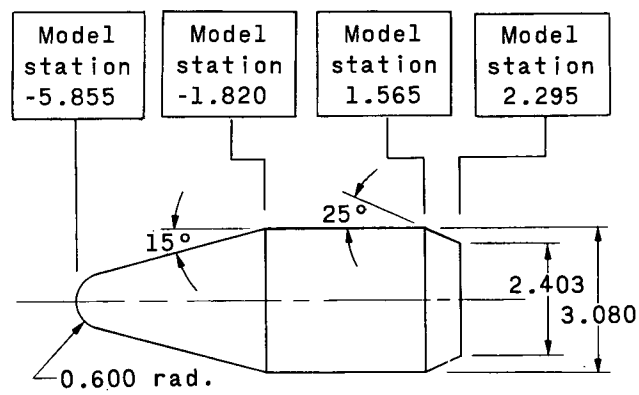

(b) Bulbous nose.

Figure 2.- Drawings of a 0.02-scale model of the Titan III launch vehicle in combination with Dyna-Soar glider and bulbous nose. All dimensions are in inches unless otherwise indicated.

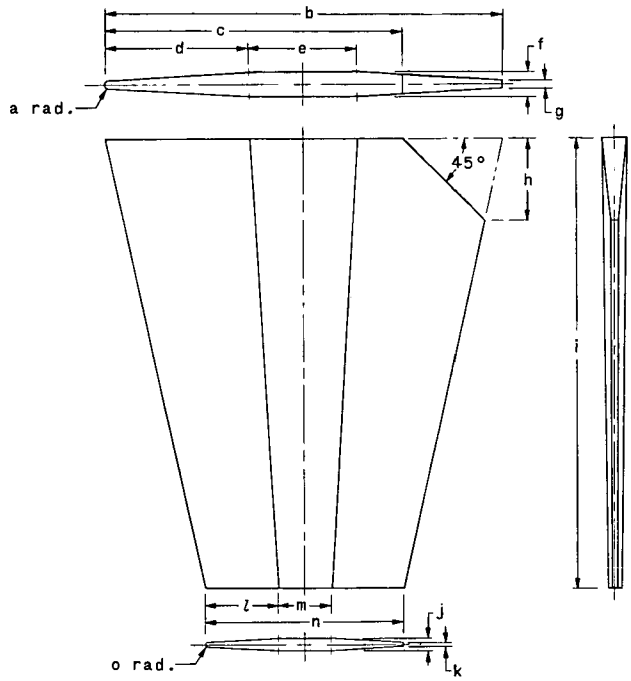

	F_{P1}	F_{P2}
a	Radius equals 0.5g	
b	3.748	4.960
c	2.820	3.730
d	1.374	1.818
e	1.000	1.324
f	0.225	0.298
g	0.075	0.099
h	0.760	1.006
i	4.220	5.580
j	0.112	0.149
k	0.037	0.050
l	0.687	0.909
m	0.500	0.662
n	1.874	2.480
o	Radius equals 0.5k	

(c) Pitch fins.

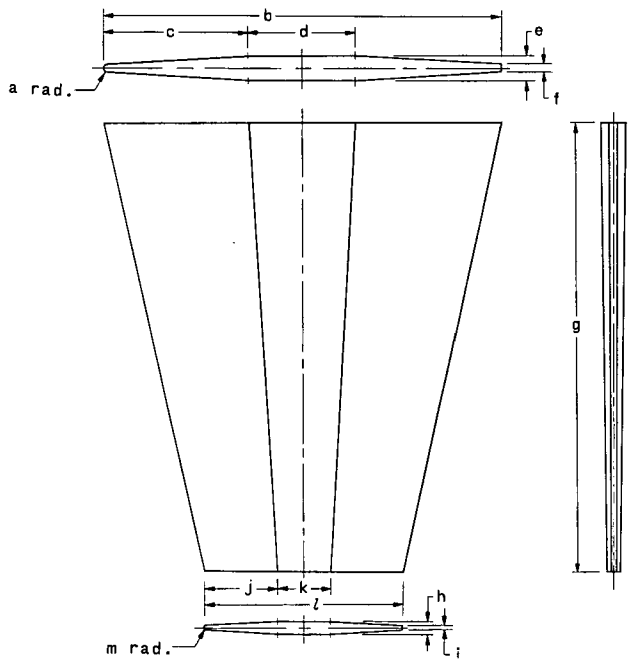

	F_{Y1}	F_{Y2}	F_{Y3}
a	Radius equals 0.5f		
b	1.482	1.960	2.160
c	0.543	0.719	0.792
d	0.396	0.522	0.576
e	0.089	0.118	0.130
f	0.030	0.039	0.043
g	1.666	2.204	2.430
h	0.044	0.059	0.065
i	0.015	0.020	0.022
j	0.272	0.359	0.396
k	0.197	0.262	0.288
l	0.741	0.980	1.080
m	Radius equals 0.5i		

(d) Yaw fins.

Figure 2.- Concluded.

L-63-3184

Figure 3.- Test-section installation of model of Titan III launch vehicle with Dyna-Soar glider and small pitch and yaw fins.

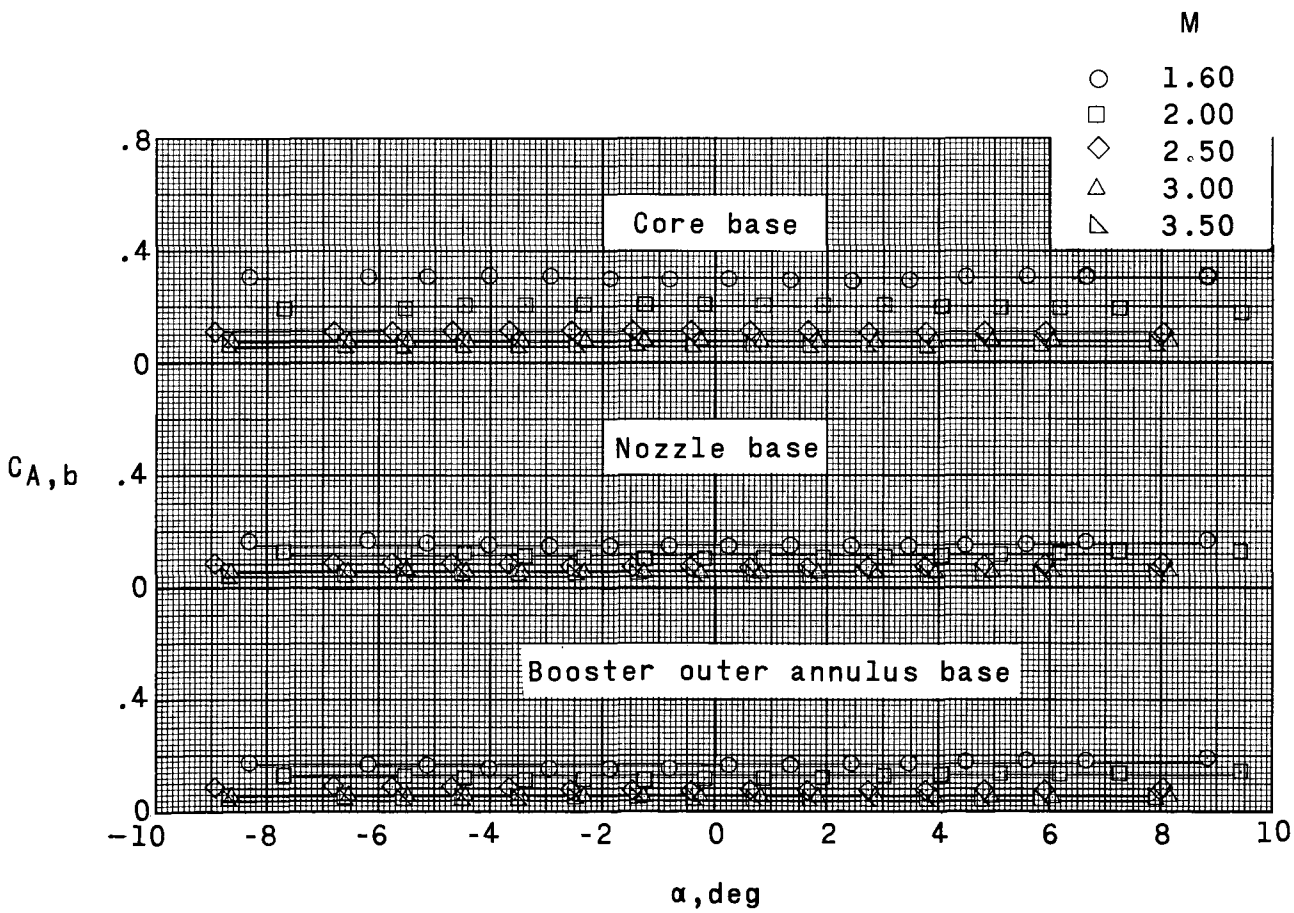

Figure 4.- Typical variation of base axial-force coefficient with angle of attack for a 0.02-scale model of the Titan III launch vehicle.

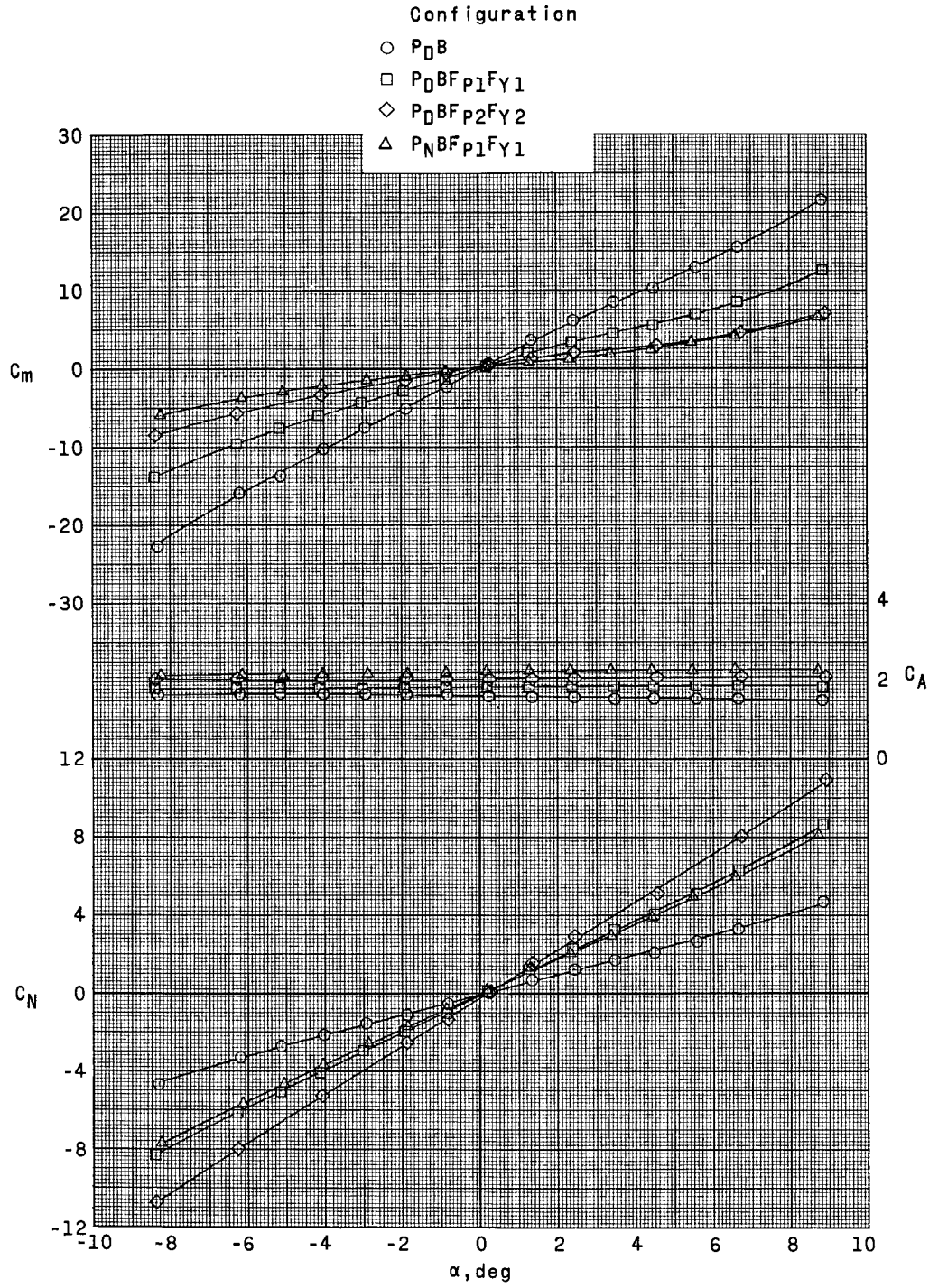

(a) M = 1.60.

Figure 5.- Aerodynamic characteristics in pitch of a 0.02-scale model of the Titan III launch vehicle with various fin arrangements and glider and bulbous nose.

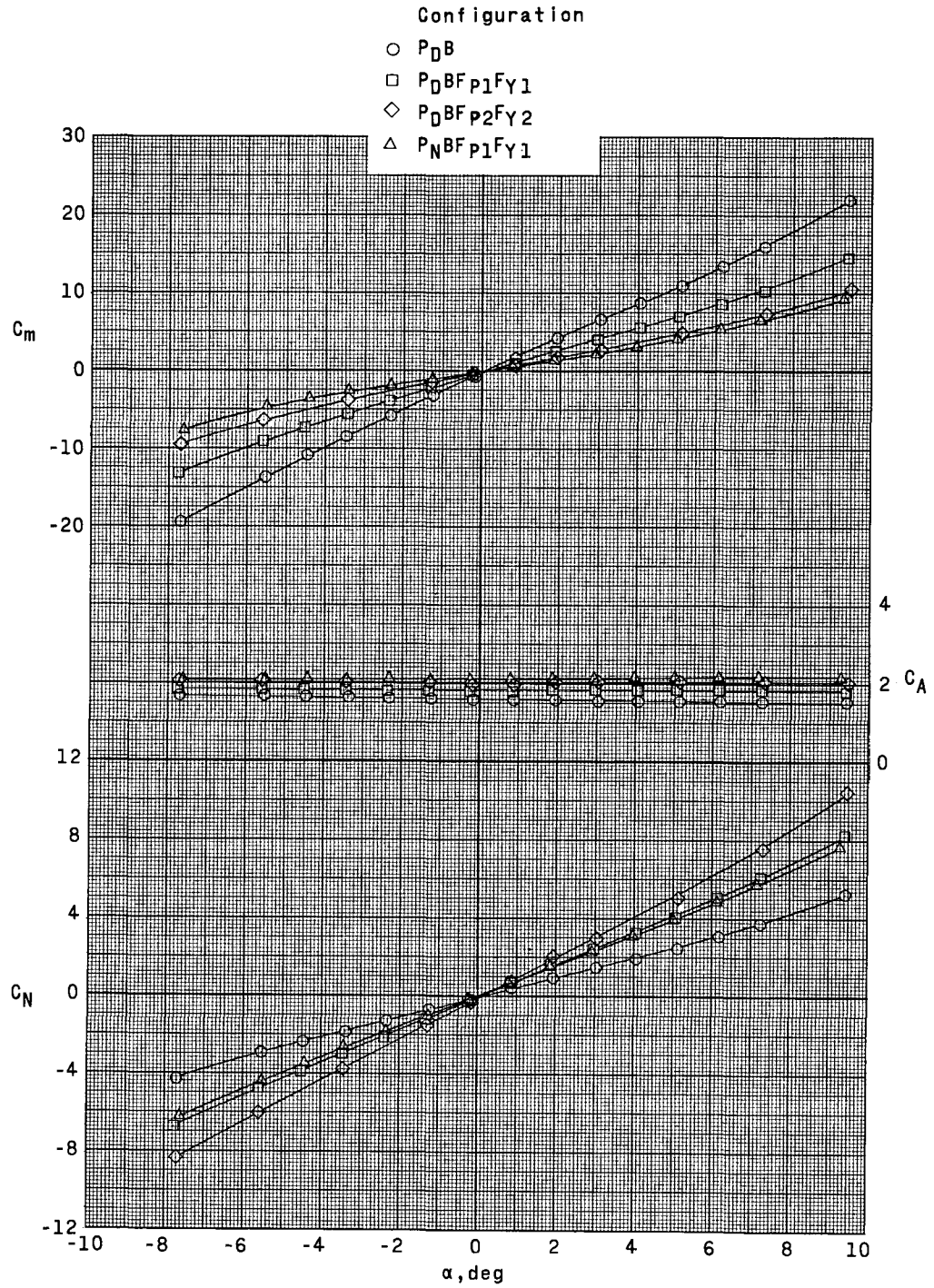

(b) M = 2.00.

Figure 5.- Continued.

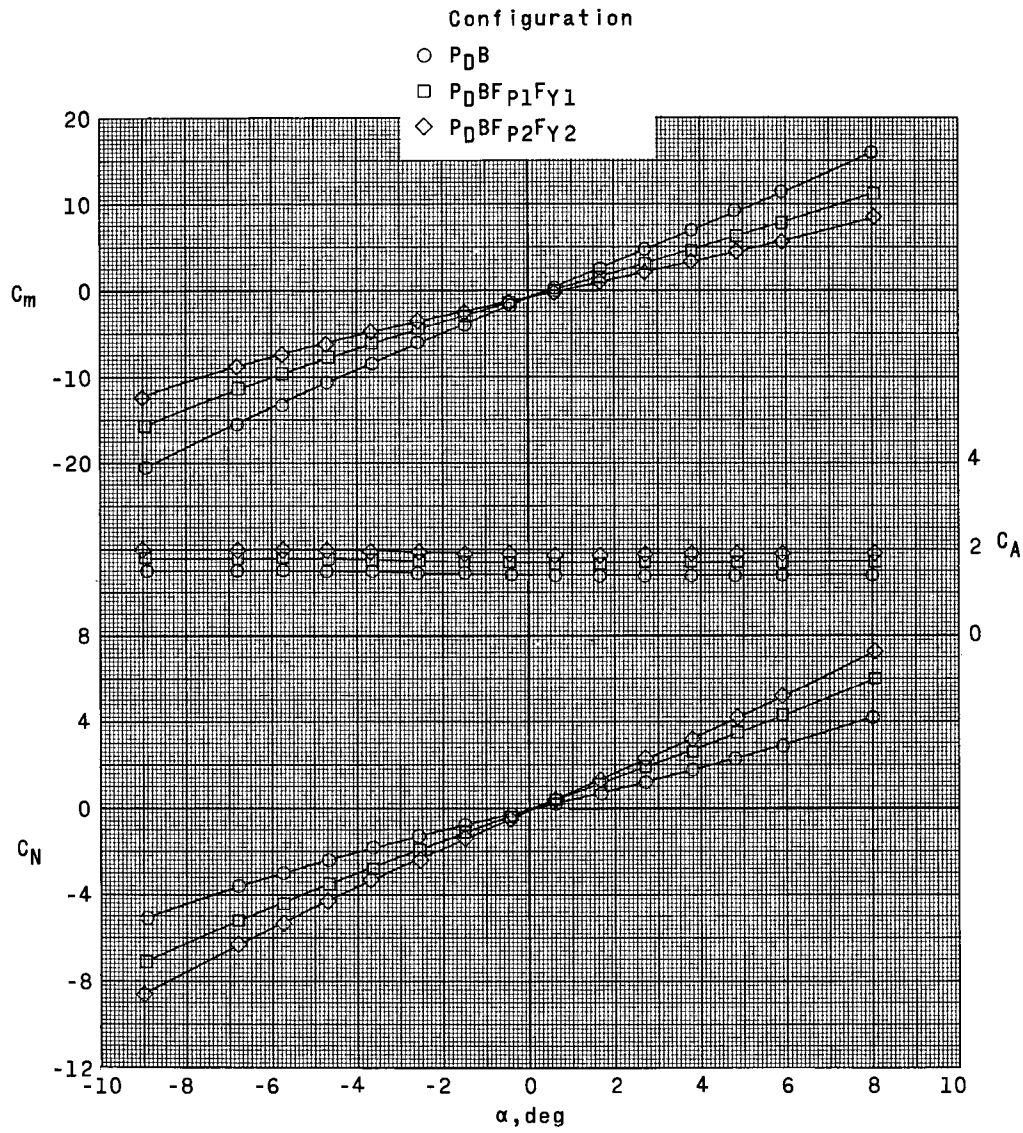

(c) M = 2.50.

Figure 5.- Continued.

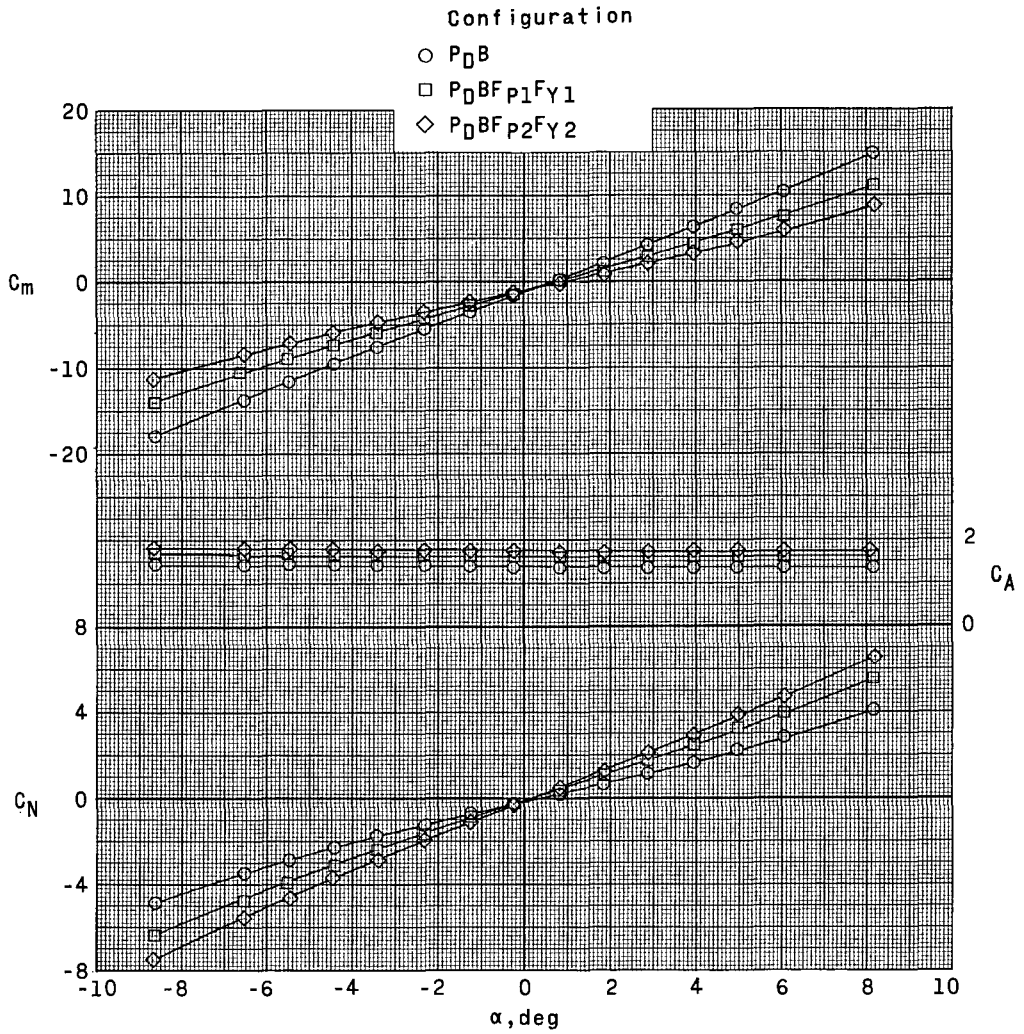

(d) M = 3.00.

Figure 5.- Continued.

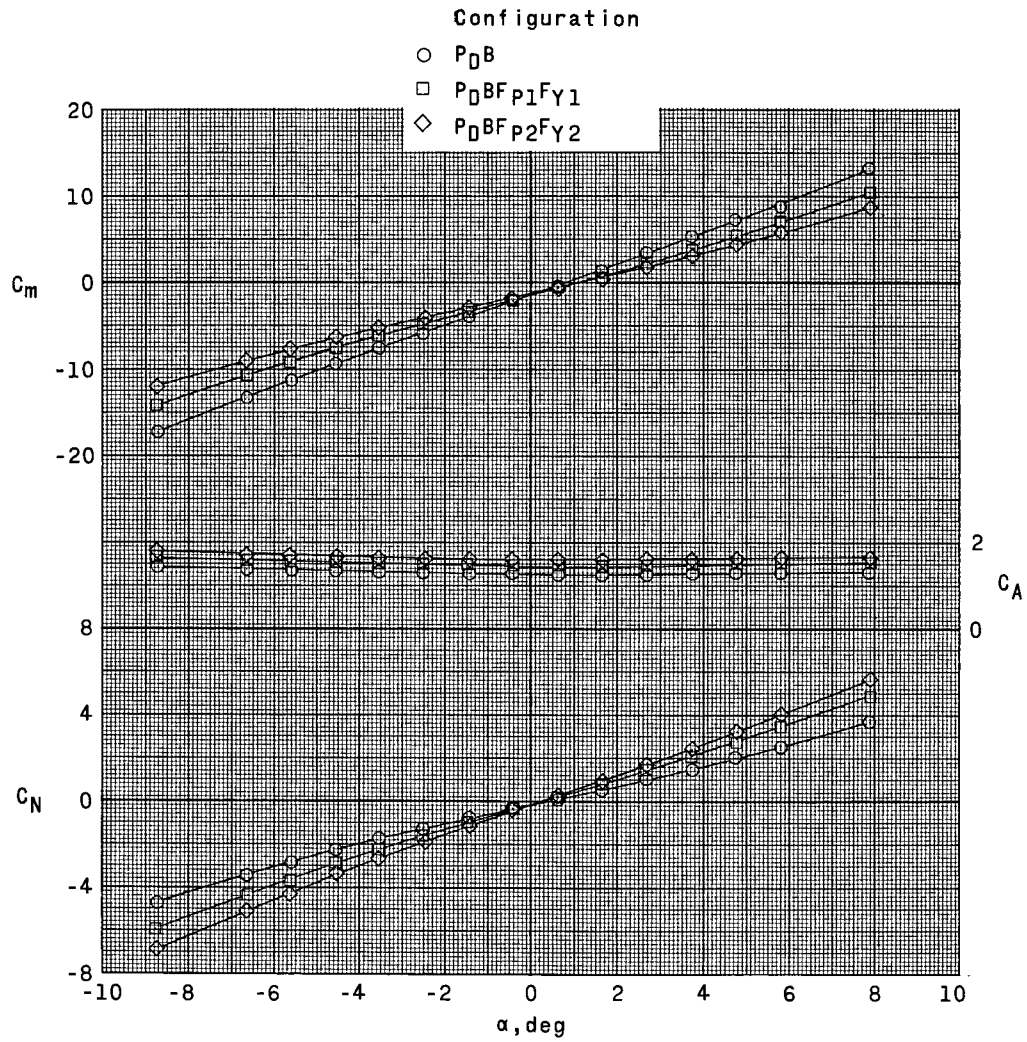

(e) M = 3.50.

Figure 5.- Concluded.

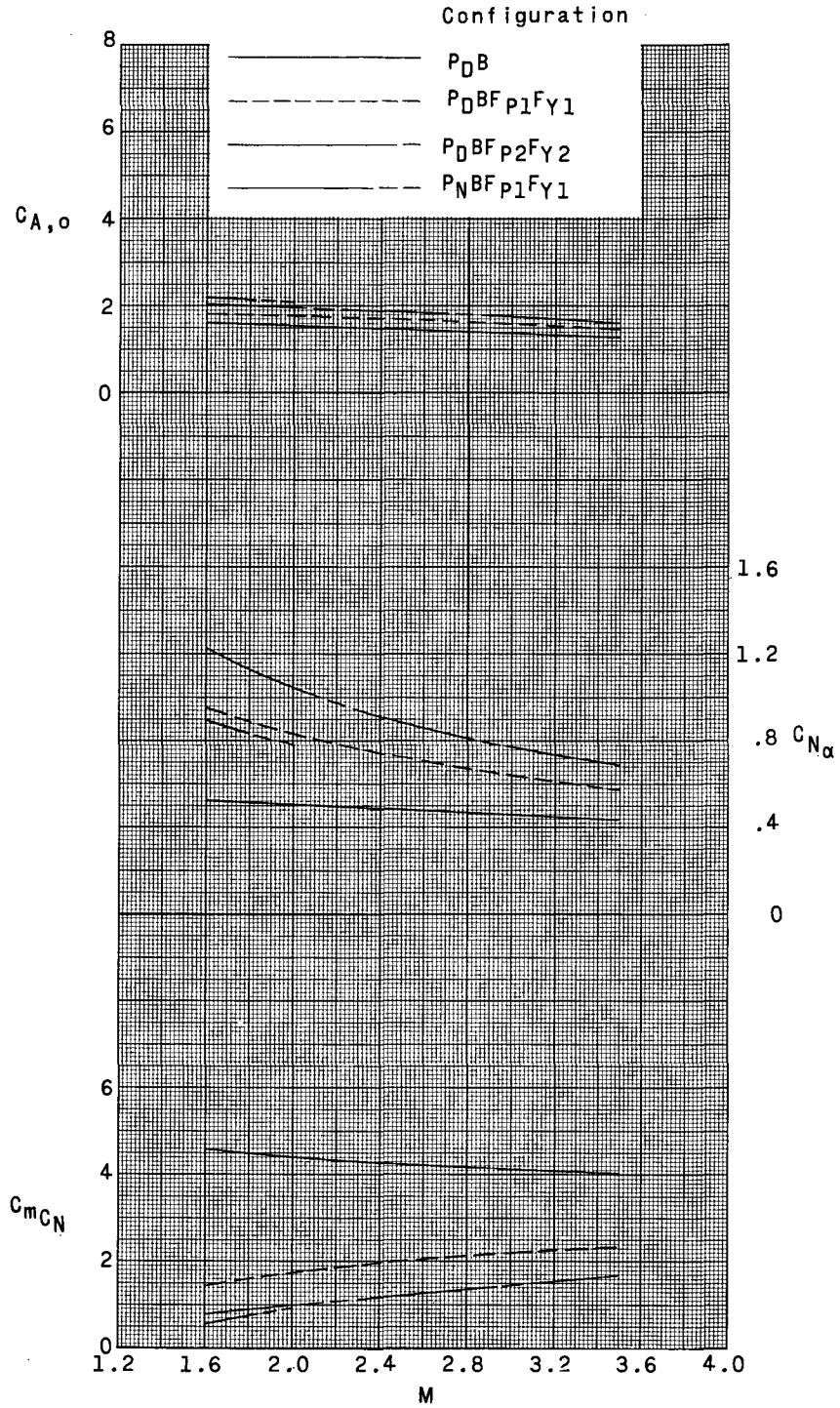

Figure 6.- Summary of the aerodynamic characteristics in pitch of a 0.02-scale model of the Titan III launch vehicle with various fin arrangements and glider and bulbous nose.

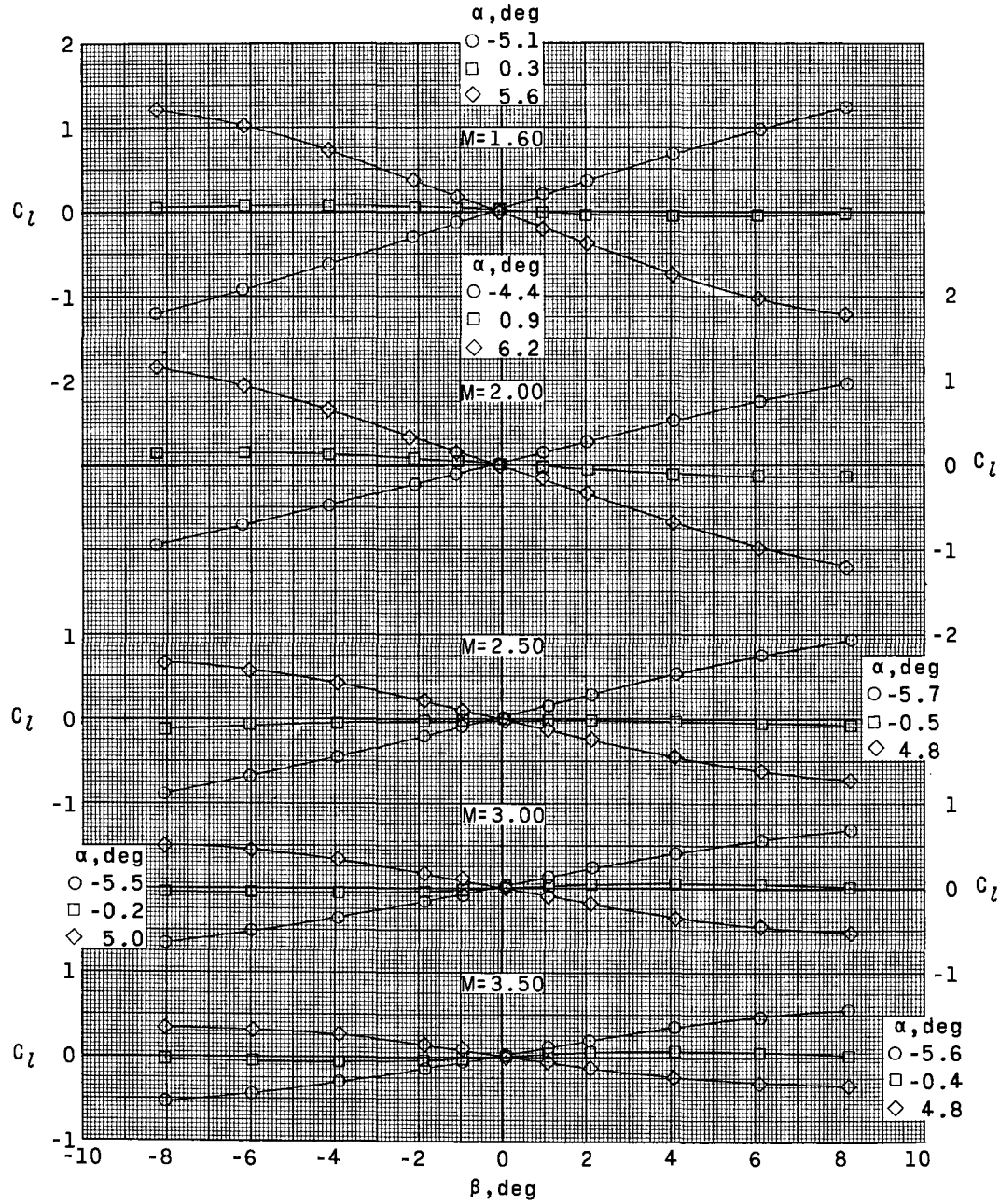

(a) Variation of C_l with β.

Figure 7.- Aerodynamic characteristics in sideslip of a 0.02-scale model of the Titan III launch vehicle and Dyna-Soar glider.

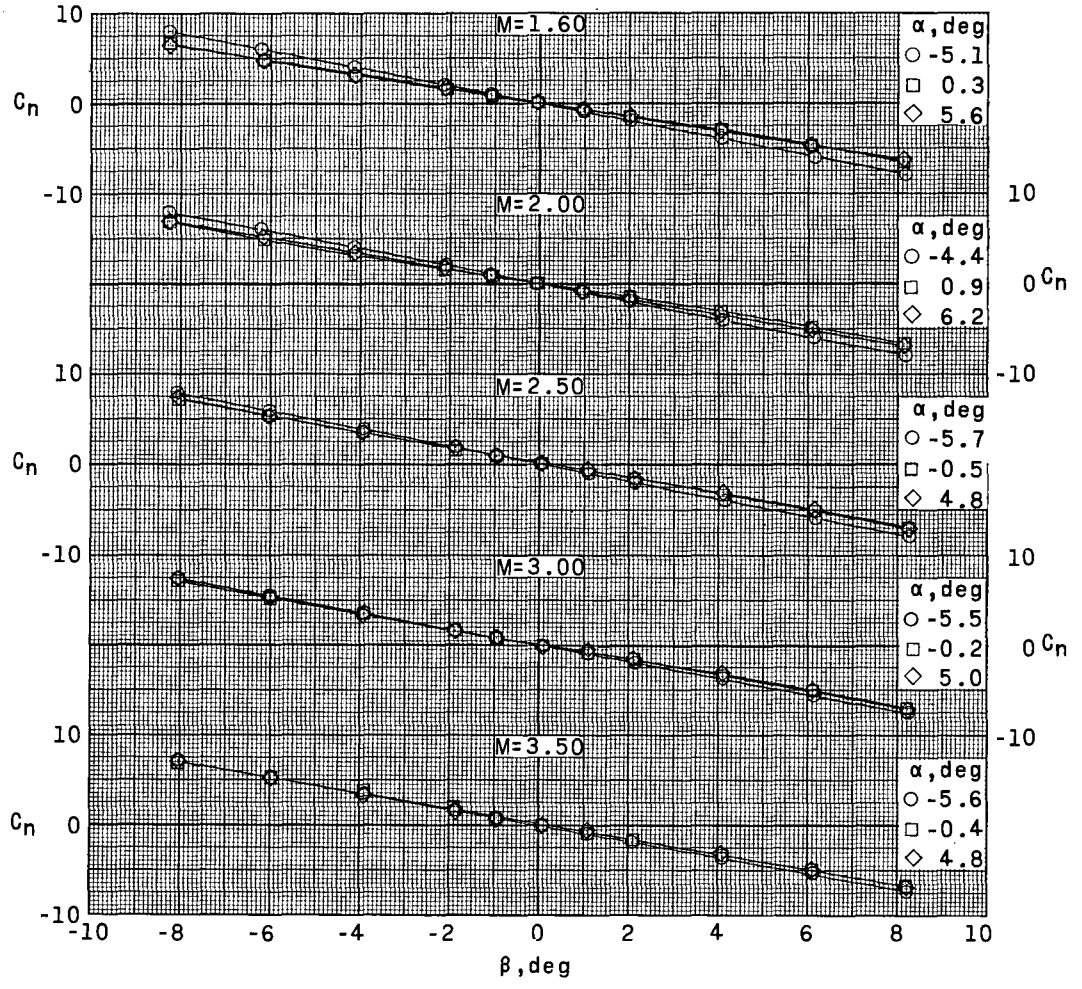

(b) Variation of C_n with β.

Figure 7.- Continued.

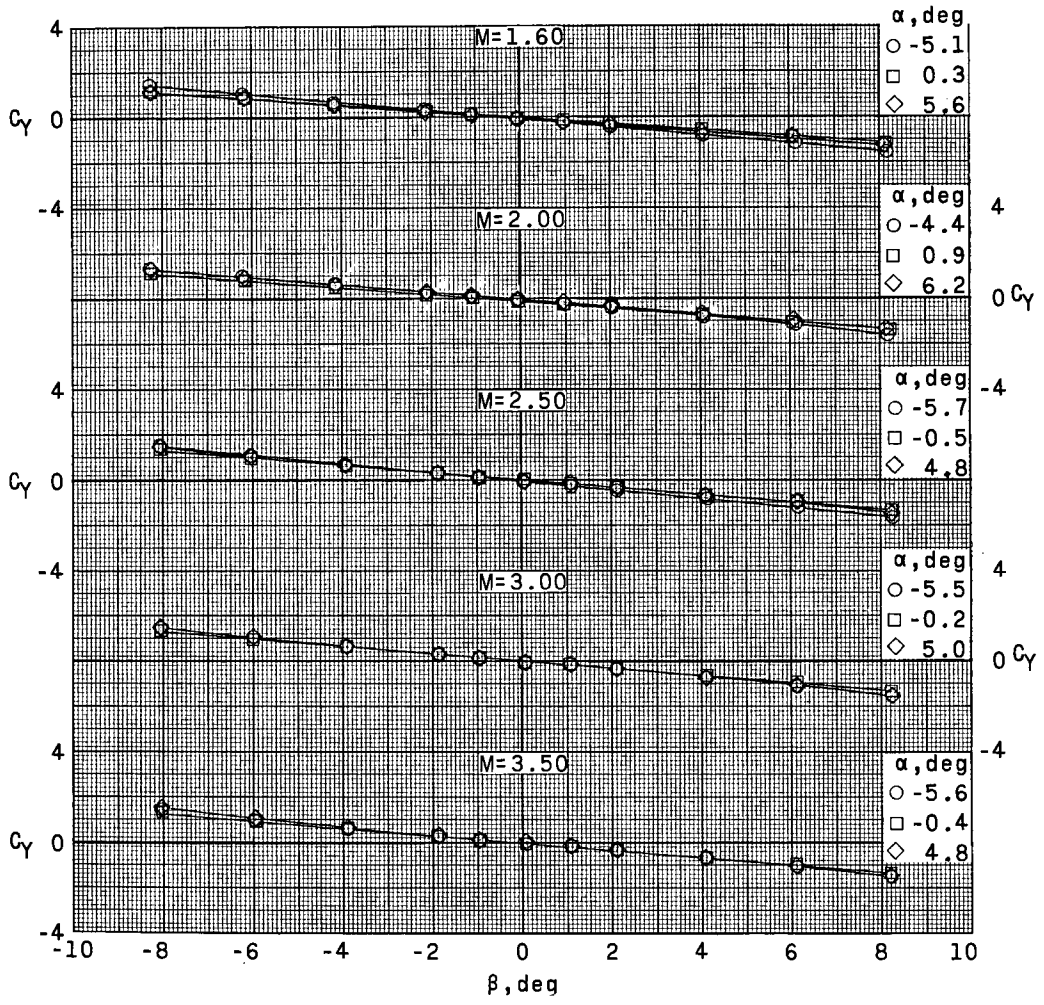

(c) Variation of C_Y with β.

Figure 7.- Concluded.

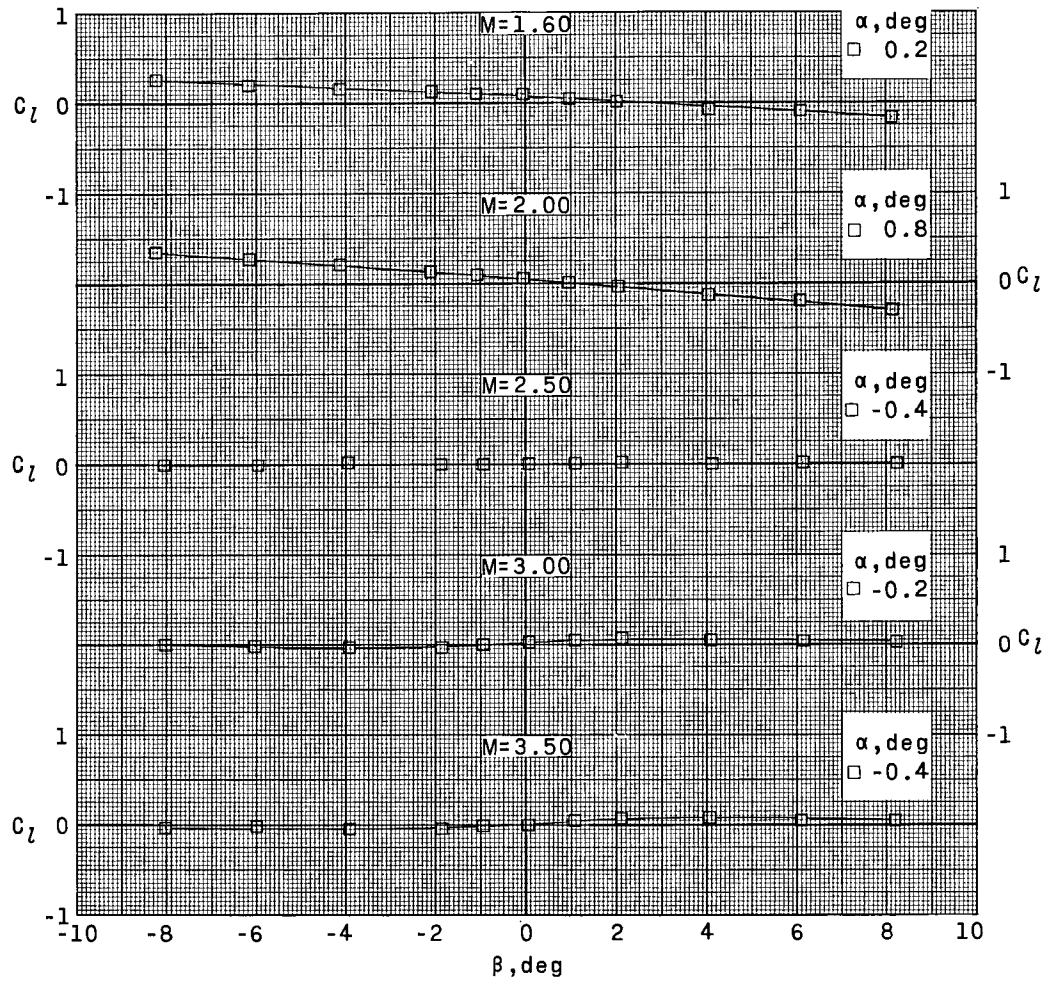

(a) Variation of C_l with β.

Figure 8.- Aerodynamic characteristics in sideslip of a 0.02-scale model of the Dyna-Soar glider and Titan III launch vehicle with small pitch and yaw fins.

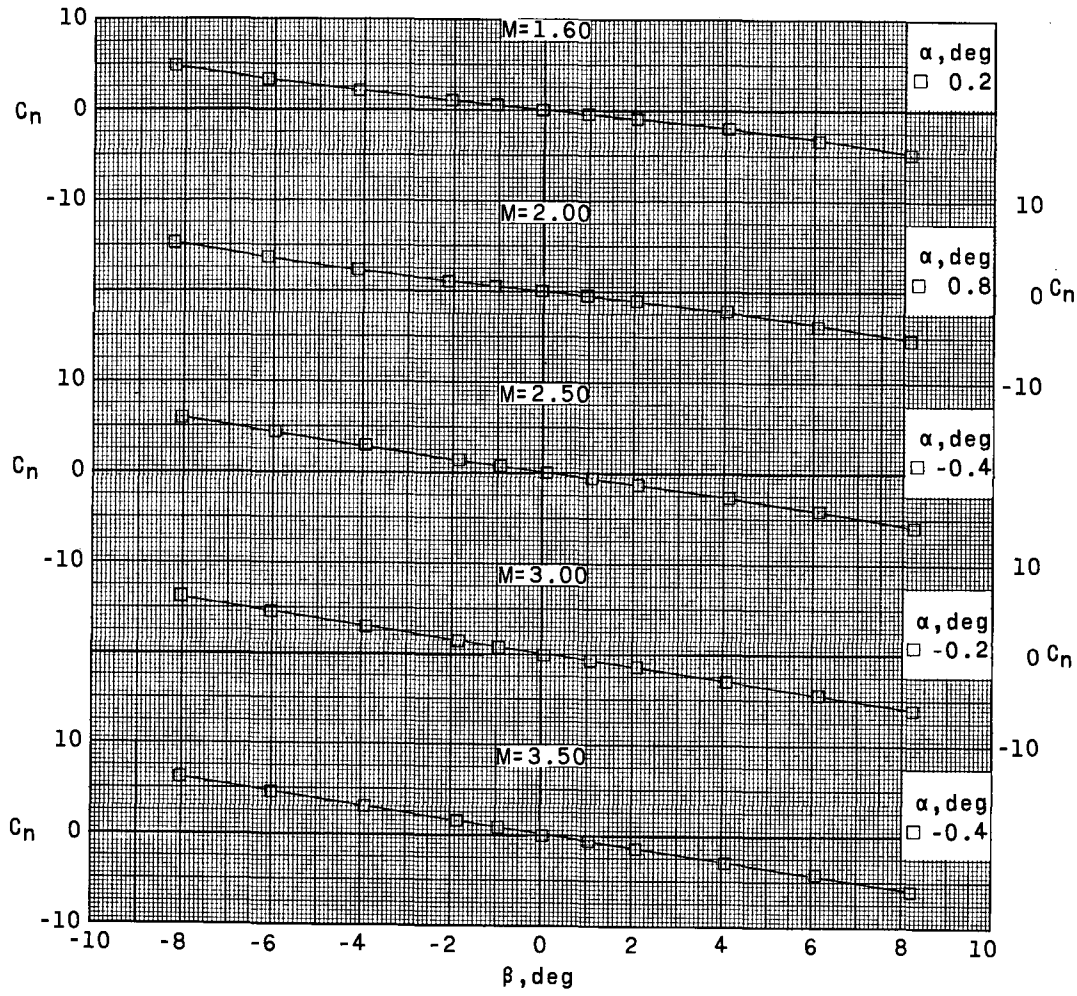

(b) Variation of C_n with β.

Figure 8.- Continued.

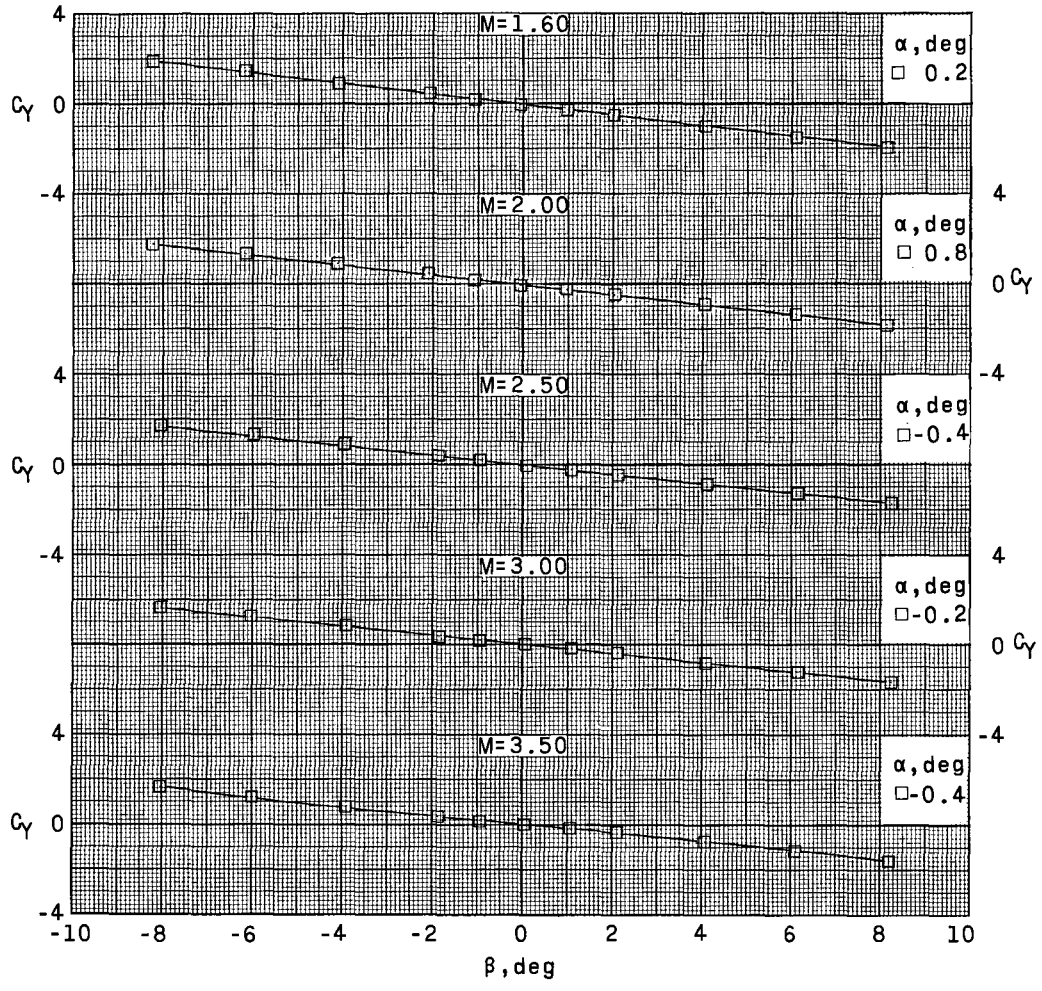

(c) Variation of C_Y with β.

Figure 8.- Concluded.

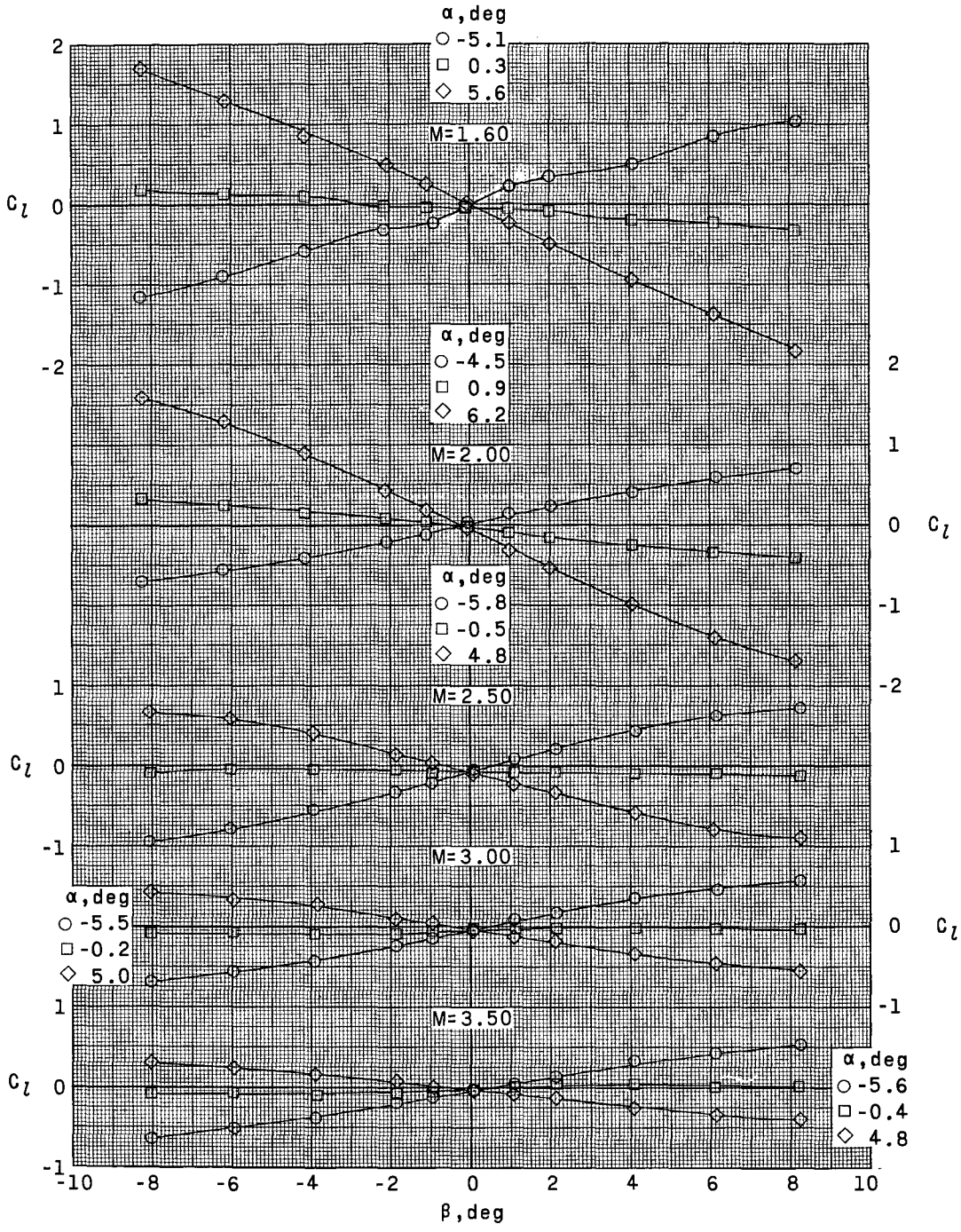

(a) Variation of C_l with β.

Figure 9.- Aerodynamic characteristics in sideslip of a 0.02-scale model of the Dyna-Soar glider and Titan III launch vehicle with large pitch fins and medium yaw fins.

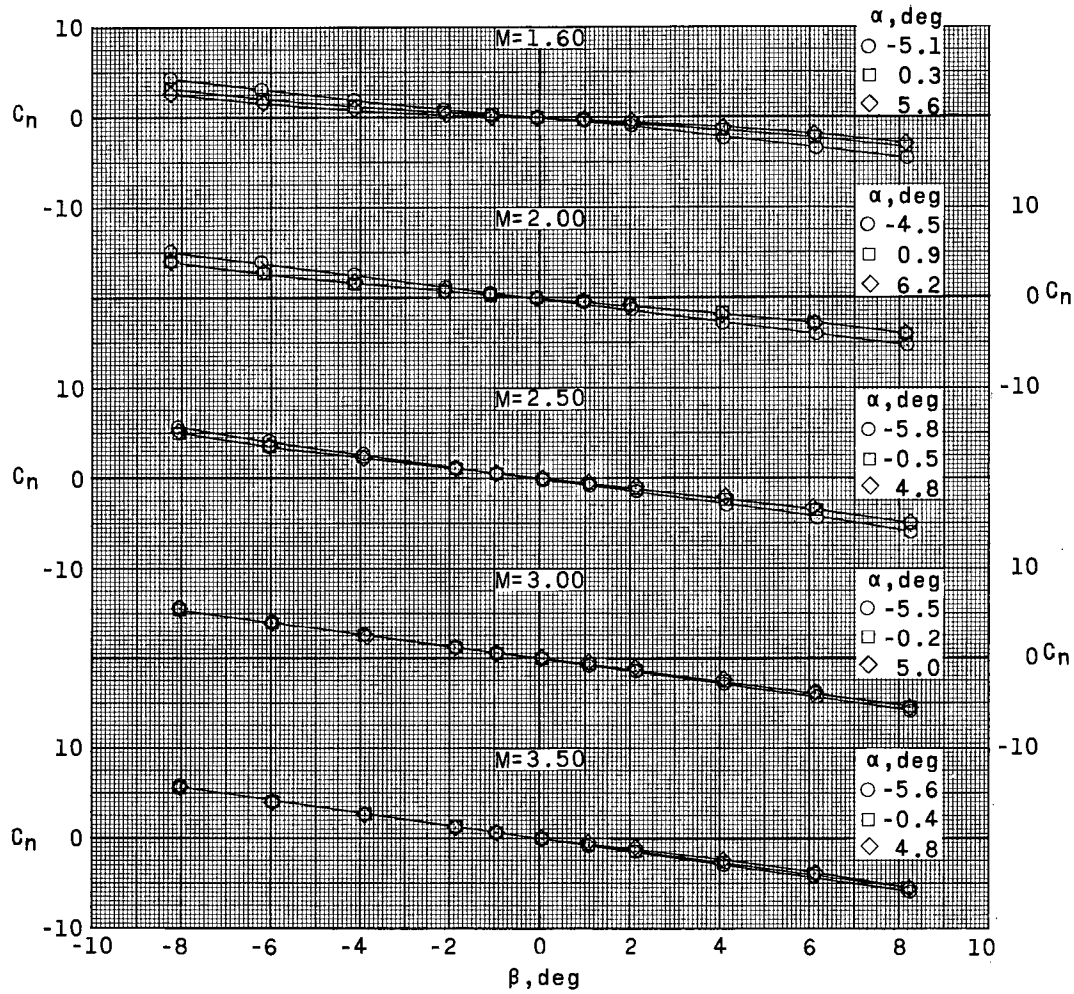

(b) Variation of C_n with β.

Figure 9.- Continued.

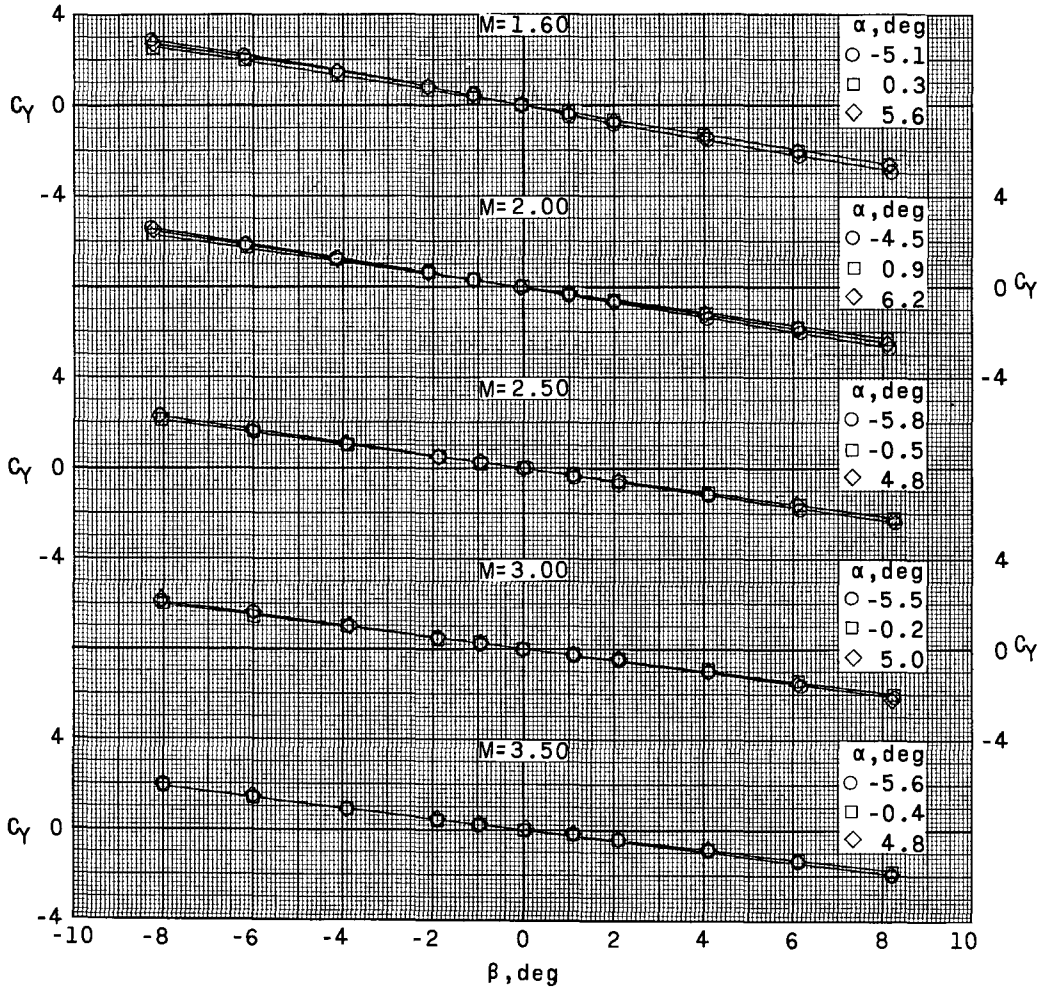

(c) Variation of C_Y with β.

Figure 9.- Concluded.

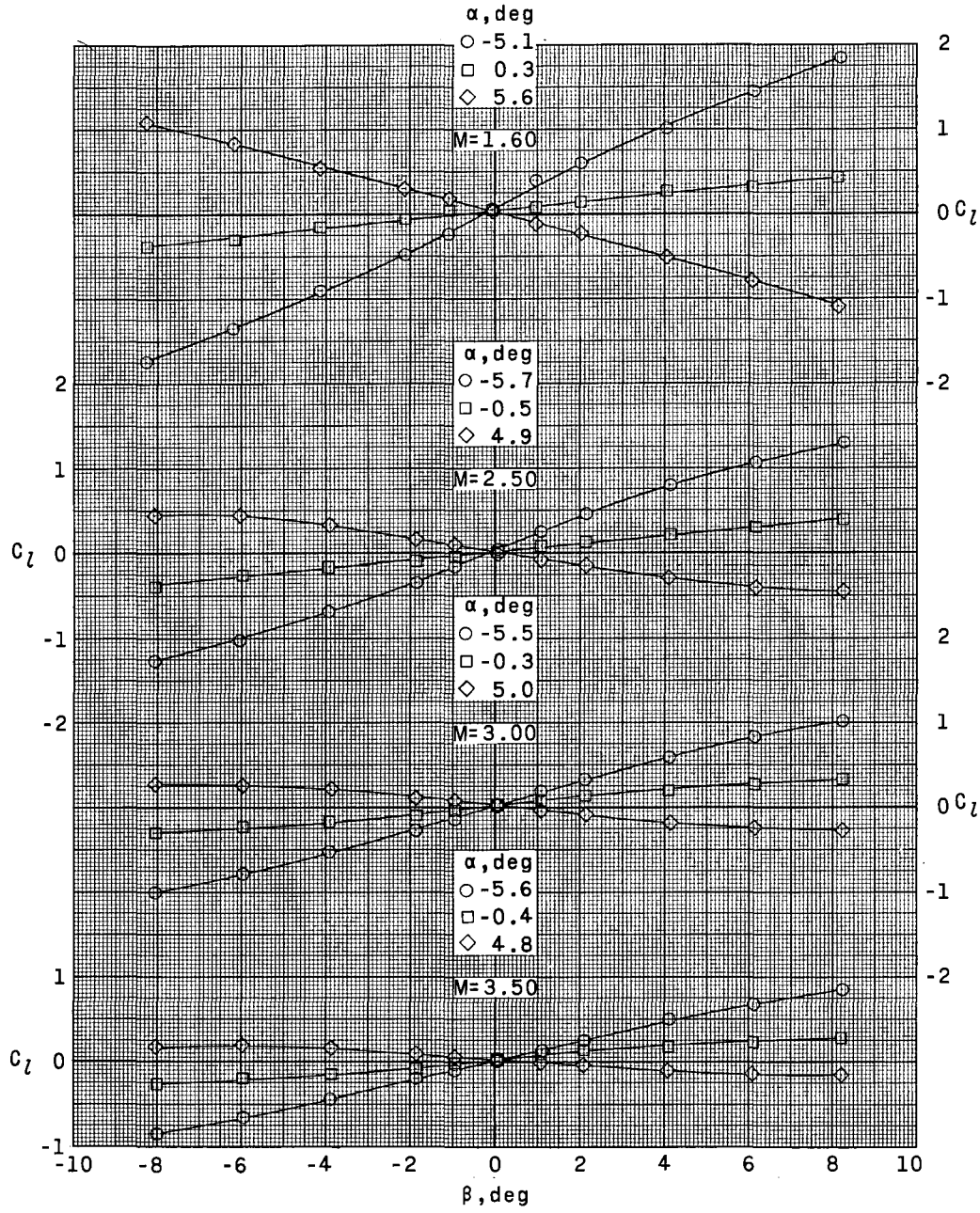

(a) Variation of C_l with β.

Figure 10.- Aerodynamic characteristics in sideslip of a 0.02-scale model of the Dyna-Soar glider and Titan III launch vehicle with small pitch fins and large yaw fins.

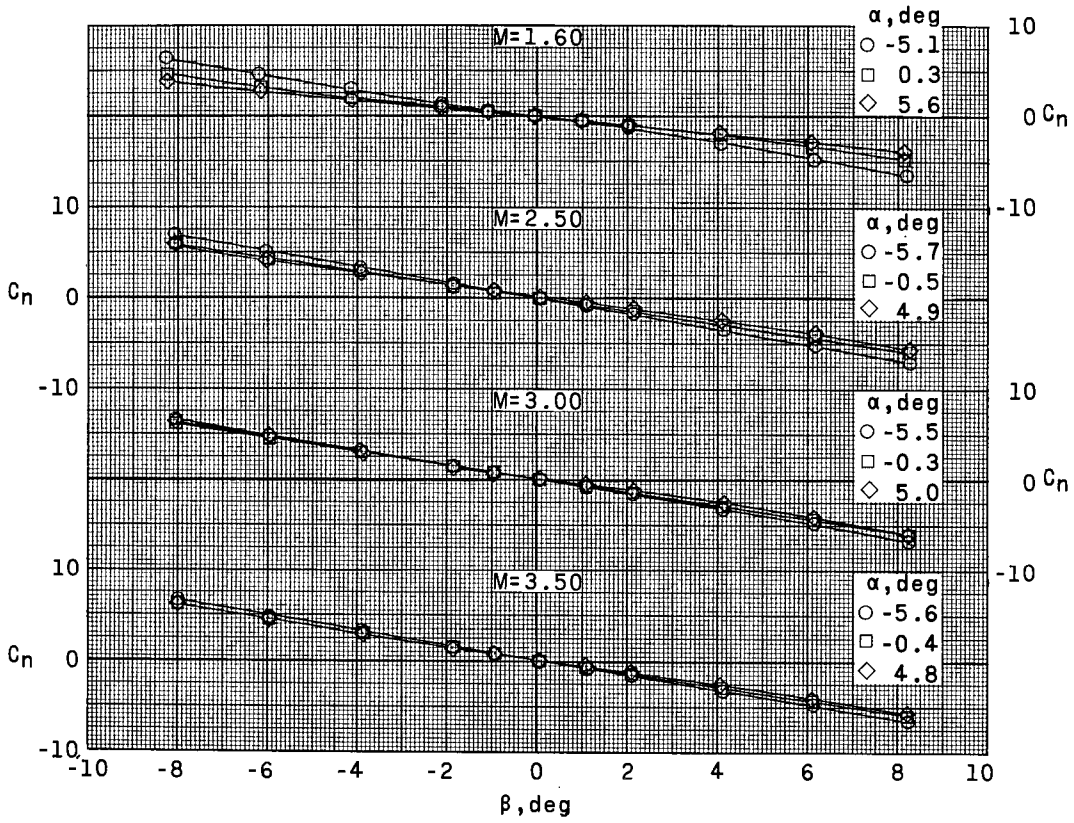

(b) Variation of C_n with β.

Figure 10.- Continued.

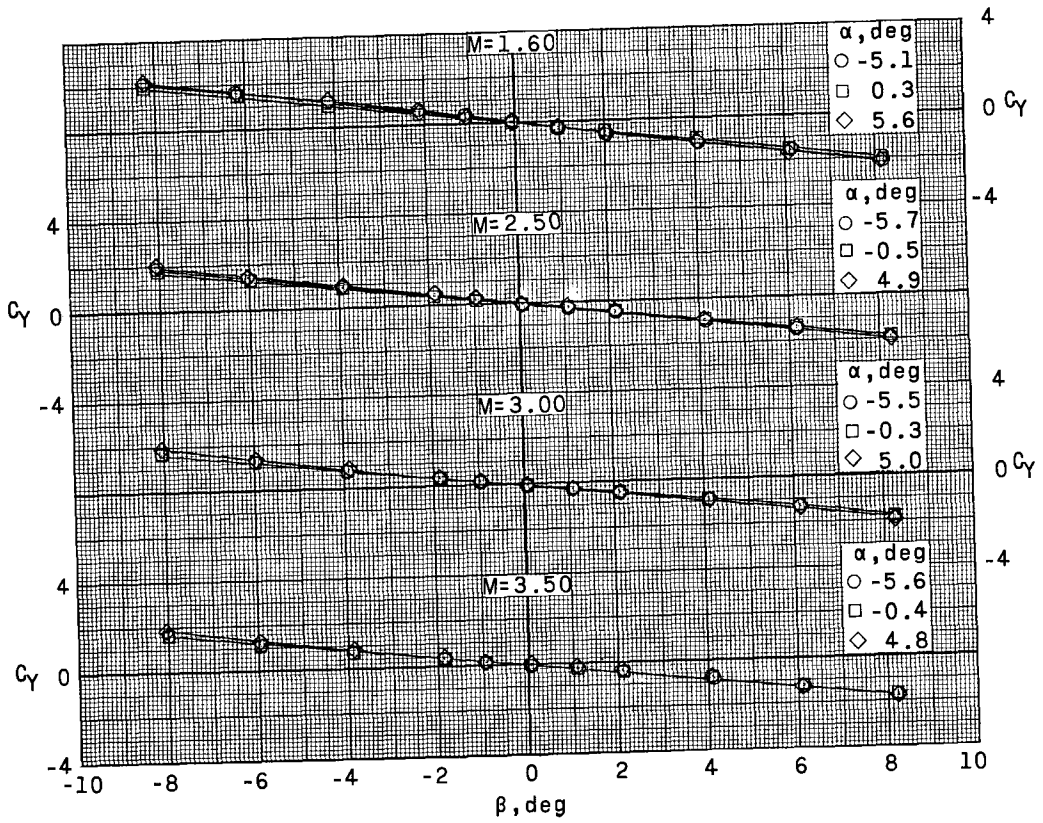

(c) Variation of C_Y with β.

Figure 10.- Concluded.

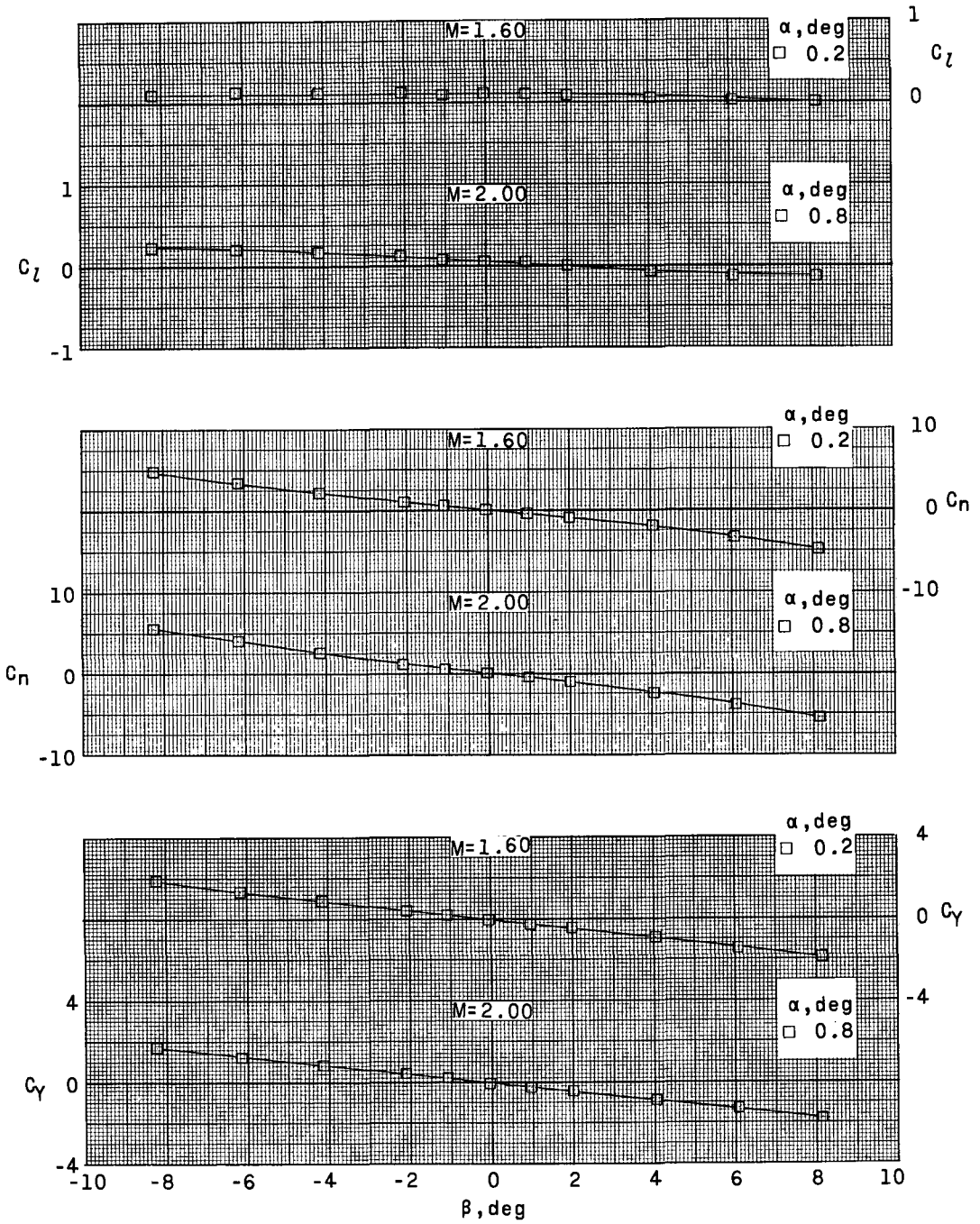

Figure 11.- Aerodynamic characteristics in sideslip of a 0.02-scale model of the bulbous nose shape and Titan III launch vehicle with small pitch and yaw fins.

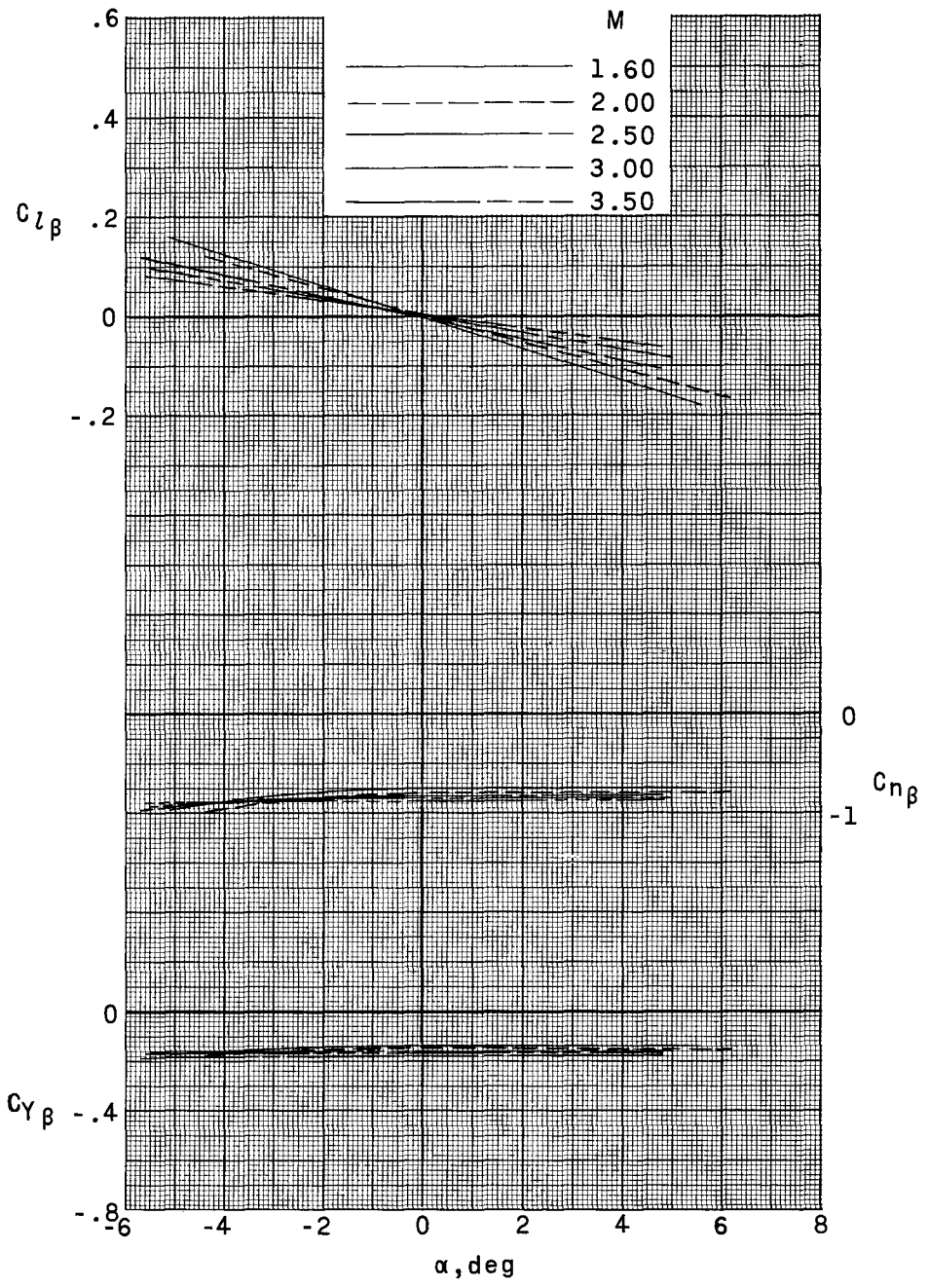

(a) Configuration P_DB.

Figure 12.- Summary of the aerodynamic characteristics in sideslip of various configurations of test model.

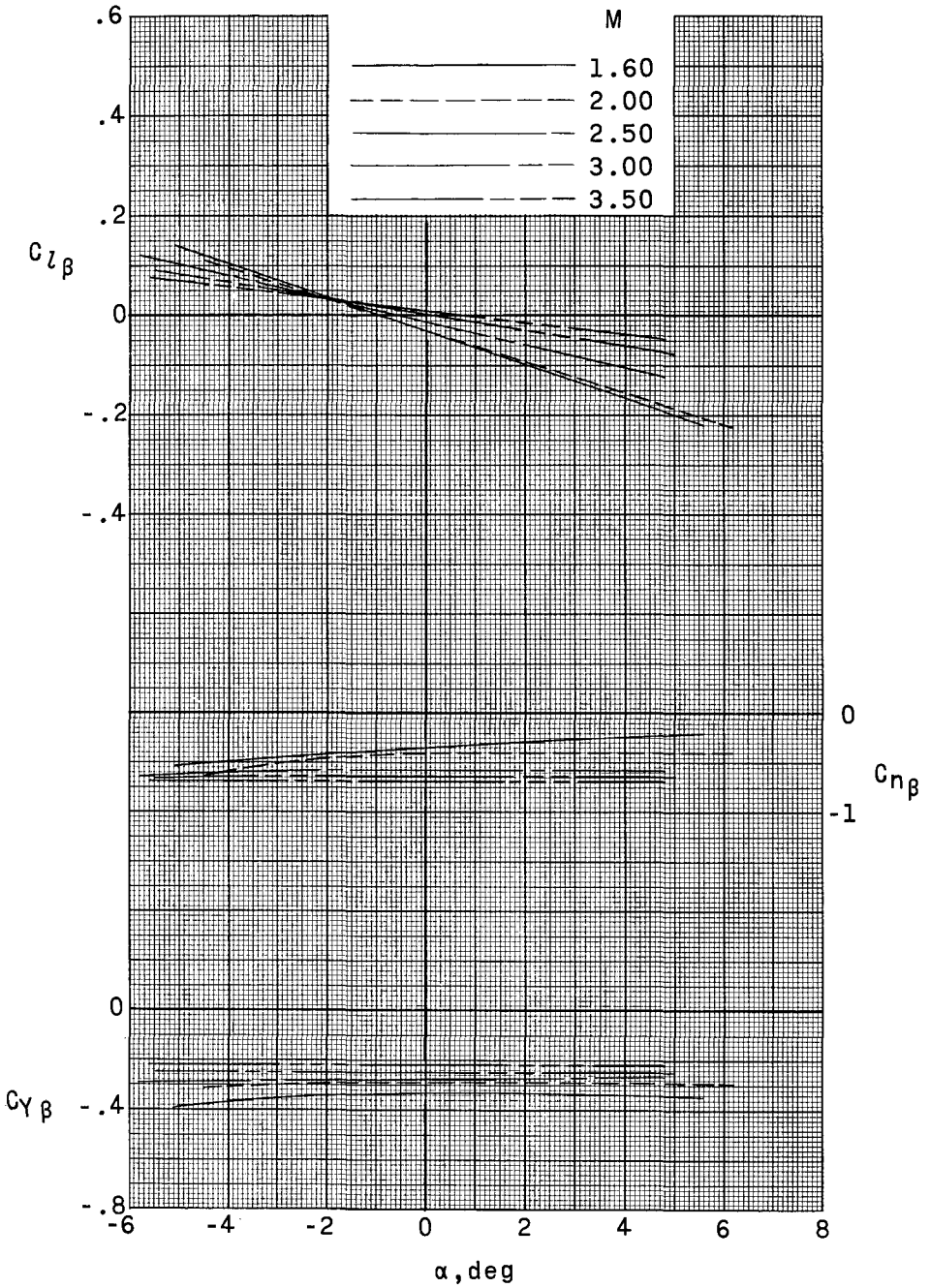

(b) Configuration $P_DBF_{P2}F_{Y2}$.

Figure 12.- Continued.

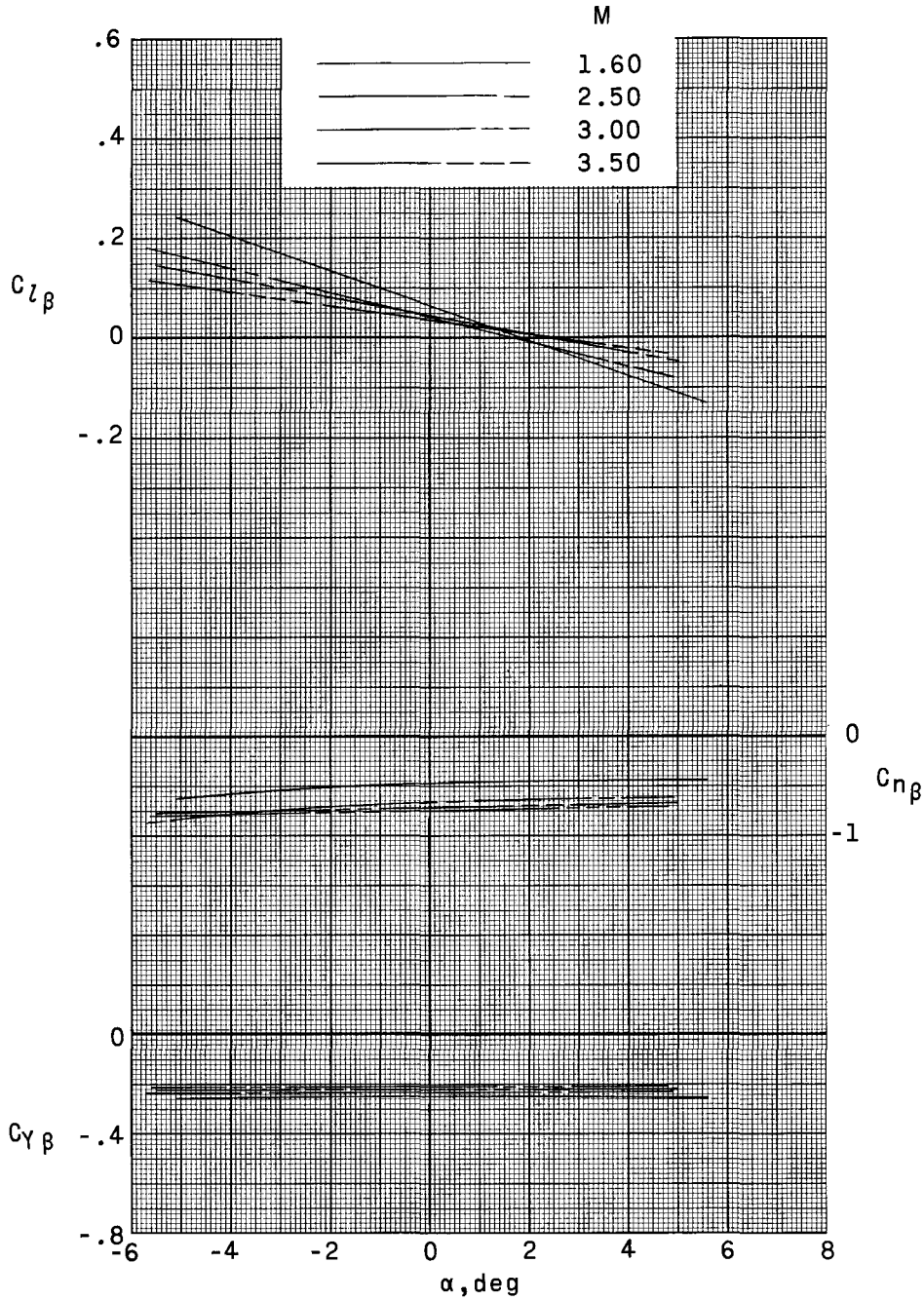

(c) Configuration $P_DBF_{P1}F_{Y3}$.

Figure 12.- Concluded.